

PCCP

Accepted Manuscript



This is an *Accepted Manuscript*, which has been through the Royal Society of Chemistry peer review process and has been accepted for publication.

Accepted Manuscripts are published online shortly after acceptance, before technical editing, formatting and proof reading. Using this free service, authors can make their results available to the community, in citable form, before we publish the edited article. We will replace this *Accepted Manuscript* with the edited and formatted *Advance Article* as soon as it is available.

You can find more information about *Accepted Manuscripts* in the [Information for Authors](#).

Please note that technical editing may introduce minor changes to the text and/or graphics, which may alter content. The journal's standard [Terms & Conditions](#) and the [Ethical guidelines](#) still apply. In no event shall the Royal Society of Chemistry be held responsible for any errors or omissions in this *Accepted Manuscript* or any consequences arising from the use of any information it contains.

Cite this: DOI: 10.1039/c0xx00000x

www.rsc.org/xxxxxx

ARTICLE TYPE

Questionable excited-state double-proton transfer mechanism for 3-hydroxyisoquinoline

Jinfeng Zhao^{a,b}, Yanling Cui^a, Jing Wang^a, Lixin Xia^a, Yumei Dai^d, Junsheng Chen^b, Peng Song^{a,c*} and Fengcai Ma^{a,c*}

Received (in XXX, XXX) XthXXXXXXXXXX 20XX, Accepted Xth XXXXXXXXXXXX 20XX

DOI: 10.1039/b000000x

Two excited state proton transfer mechanisms of 3-hydroxyisoquinoline (3HIQ) in cyclohexane and acetic acid (ACID) were investigated based on the time-dependent density functional theory (TDDFT), suggesting a different double-proton transfer mechanism from the one proposed previously (*J. Phys. Chem. B* 1998, 102, 1053). Instead of the formation of keto/enol complexes for 3HIQ self-association in cyclohexane, our theoretical results predicted that 3HIQ self-association exists in two forms: the normal form (enol/enol) and the tautomer form (keto/keto) in cyclohexane. A high barrier (37.023 kcal/mol) between the 3HIQ enol monomer and 3HIQ keto monomer form indicated that the 3HIQ keto monomer in the ground state should not exist. In addition, the constructed potential energy surfaces of the ground state and excited state have been used to explain the proton transfer process. Upon optical excitation, the enol/enol form is excited to the first excited state, then transfers one proton, in turn, transition to the ground state to transfer another proton. A relatively low barrier (8.98 kcal/mol) demonstrates two stable structures in the ground state. In view of the acetic acid solvent effect, two protons of 3HIQ/ACID transfer along the dihydrogen bonds in the first excited state, which is a different transfer mechanism to 3HIQ self-association. In addition, the proton transfer process provides a possible explanation for the fluorescence quenching observed.

1. Introduction

It is well known that the phenomenon of hydrogen bonding has been recognized for its importance in physics, chemistry, and biology in recent years^[1–11]. Up to now, many different sensing mechanisms, such as photoinduced electron transfer (PET), intramolecular charge transfer (ICT), excited state proton transfer (ESPT), and fluorescence resonance energy transfer (FRET) have been explained reasonably via hydrogen bond interactions^[12–20]. Proton transfer (PT) is one of the most important reactions in chemical and biological acid–base dynamics resulting from site-specific interactions through hydrogen bonding^[21–24]. The study of excited-state intramolecular and intermolecular proton transfer (ESIPT) processes has been an active area of research since the

first experimental observation of the phenomenon by Weller *et al.* in the middle of the last century^[25]. PT occurs in molecules containing both acidic and basic groups in close proximity that may rearrange in the excited electronic state via a proton or hydrogen atom transfer. And more and more materials and biological systems, containing two protons, are of special interest recently. Lischka and co-workers reported an excited-state double proton transfer reaction in [2,2'-Bipyridyl]-3,-3'-diol, and the sequential proton transfer mechanism was concluded^[26]. The excited-state double proton transfer reaction of 2-aminopyridine/acid system were reported by Han and co-workers, which demonstrated the important role of the intermolecular hydrogen bonding between 2-aminopyridine and acid^[27]. Particularly, they provided the method of potential energy curves to explain the double proton transfer mechanism for the first time based on the TDDFT method^[27]. In a word, the strong and fast reorganization of the charge distribution derived from the proton transfer tautomerization makes these molecules very attractive towards the design and use of fluorescence sensors^[28–33], laser dyes and LEDs^[34, 35], UV filters^[36–38], and molecular switches^[39, 40]. In fact, excited state intramolecular, as well as intermolecular proton transfer is one of the simplest examples of a hydrogen bond reaction that occurs in an electronically excited molecule. Upon photoexcitation, the molecules can be projected

^a College of Physics and College of Chemistry, Liaoning University, Shenyang 110036, P. R. China E-mail: songpeng@lnu.edu.cn; fema@lnu.edu.cn

^b State Key Lab of Molecular Reaction Dynamics, Dalian Institute of Chemical Physics, Chinese Academy of Sciences, Dalian 116023, China

^c Liaoning Key Laboratory of Semiconductor Light Emitting and Photocatalytic Materials, Liaoning University, Shenyang 110036, P. R. China

^d Normal College, Shenyang University, Shenyang 110044, P. R. China

on a potential energy surface that can make the position of a proton unstable. The energy difference between the locally excited and relaxed excited state provides the driving force for the transformation, and in turn, the slope of the surface connecting these two points determines the relative kinetics. In fact, stationary fluorescence spectroscopy provides important indications of the occurrence of proton transfer in the excited state. The observation of a nearly mirror symmetry between absorption and fluorescence spectra indicates that, over the timescale of the excited state lifetime, the nuclear configuration of the molecule and its surrounding medium remains close to that of the ground state, while the influence of the proton transfer on the Frank-Condon factors is enough to result in the break-up of the mirror symmetry. The light fluorescence originating from a proton-transferred state occurs at a longer wavelength with a red shift with respect to absorption ranging. It is therefore possible to interpret the normal, shorter wavelength fluorescence as originating from the locally excited state, and to associate the red shifted long wavelength fluorescence with the product of proton transfer.

Hydroxyquinoline and its derivatives have attracted interest from both chemists and biologists over the past decade^[41, 42]. The proton transfer behavior along the hydrogen bonded wire of 6-hydroxyquinoline in acetic acid (ACID) has been deliberated by Mehata *et al.*^[41]. Similarly, Chou *et al.* investigated the proton transfer of 7-hydroxyquinoline (7HQ) through hydrogen-bond formation in ACID in the ground as well as in the excited state^[42]. In addition, Liu *et al.* reported the excited-state proton transfer dynamics of the 7HO-(NH₃)₃ cluster, which revealed a more detailed mechanism for the excited-state reaction of the 7HO-(NH₃)₃ cluster^[43]. 3-Hydroxyisoquinoline (3HIQ) is considered as a prototype for the lactam-lactimtautomerism of nitrogen-containing heteroaromatic systems, and as such it has been investigated since the 1960s^[44, 45]. In fact, the 3HIQ molecule could be used as an inhibitor of hepatitis C virus RNA polymerase^[46], and the derivatives of 3HIQ are important reactants and intermediates in the synthesis of some chemical catalysts^[47]. In addition, 3HIQ, similar to 2-pyridone, is a DNA base analogue, which can be used as a prototype for investigating the influence of the electronic structure of DNA bases^[48]. Therefore it is very important to study the nature of 3HIQ in detail. Wei *et al.* studied the proton transfer tautomerism based on absorption titration experiments, steady-state and time resolved fluorescence measurements^[49]. They reported the conjugated dual hydrogen-bond effect in both ground and excited state of 3HIQ. They concluded 3HIQ self-association in cyclohexane displayed two structures in the ground state: one the enol/enol, and the other the keto/enol structure^[49]. However, in order to form the keto form, 3HIQ needs to cross a high barrier from the enol form, which is difficult to cross. Therefore, the keto/enol structure is questionable in the ground state. Based on the high barrier, 3HIQ is expected to exist as another structure rather than the keto/enol form. In addition, not only the calculation method (RHF/6-31G*) is rough, but they also ignored the solvation effects in the process of theoretical calculations. Moreover, spectroscopic techniques such as time resolved fluorescence spectroscopy, provide only indirect information about the photophysical properties and geometries. In order to give a clear

and detailed picture of this proton transfer mechanism, in the present work, a theoretical investigation based on density functional theory (DFT) and time-dependent density functional theory (TDDFT) methods have been applied to study both the ground and excited state of the molecule relevant to the transfer mechanism, respectively. We optimized the configurations of the ground states and the first excited state, and further calculated and analyzed the vertical excitation energies, frontier molecular orbitals, homologous ground-state (S₀) and the first excited state (S₁) potential energy surfaces (PES) of the 3HIQ dimer and 3HIQ-acetic acid (3HIQ/ACID) to provide direct information on the ESPT process.

2. Computational details

In the present work, all the theoretical calculations presented were accomplished using DFT and TDDFT methods with Becke's three-parameter hybrid exchange function with the Lee-Yang-Parr gradient-corrected correlation functional (B3LYP)^[50-52] as well as triple- ζ valence quality with one set of polarization functions (TZVP)^[53, 54] basis set by Gaussian 09 programs^[55]. Considering that the experiments were conducted in a solvent, in all calculations the solvent effects (cyclohexane and ACID) were based on the Polarizable Continuum Model (PCM) using the integral equation formalism variant (IEF-PCM)^[56-59]. The S₀ geometries for the 3HIQ monomer, 3HIQ self-association and 3HIQ/ACID were optimized without constrain of bonds, angles and dihedral angles. In addition, all the calculations below base on the no constraints beginning with the geometric optimization. Vibrational frequency calculations have been used to analyze the optimized structures to confirm that these structures corresponded to the local minima on the S₀ PES (no imaginary frequency). The calculations of vertical excitation energies have also been performed from the ground-optimized structure based on TDDFT methodology with IEF-PCM, and our theoretical calculations predicted the six low-lying absorbing transitions. In view of the ground equilibrium geometries, the S₁ geometries were optimized without constraint and investigated using the TDDFT method with B3LYP functional and TZVP basis set, which have been widely applied for molecule systems including weakly interacting systems^[60, 61]. Vibrational frequencies were also analyzed for the optimized structures to confirm that these structures corresponded to the local minima on the S₁ PES. All the local minima were confirmed by the absence of an imaginary mode in the vibrational analysis calculations. The S₀ and S₁ PESs of the 3HIQ monomer have been scanned by constrained optimizations and frequency analyses to obtain the thermodynamic corrections in the corresponding electronic state, and keeping the O-H distance fixed at a series of values. In turn, the S₀ and S₁ PESs of 3HIQ self-association and 3HIQ/ACID have also been scanned based on similar methods.

Fine quadrature grids of size 4 were employed. The self-consistent field (SCF) convergence thresholds of the energy for both the ground state and excited state optimization were set at 10⁻⁸ (default settings are 10⁻⁶). Harmonic vibrational frequencies in the ground and excited state were determined by diagonalization of the Hessian. The excited-state Hessian was obtained by numerical differentiation of the analytical gradients using central differences and default displacements of 0.02 Bohr.

The infrared intensities were determined from the gradients of the dipole moment ^[62].

3. Results and discussion

3.1 The 3HIQ monomer

In order to analysis the balanceable structures of 3HIQ self-association in the ground state, it is necessary to investigate the 3HIQ monomer first. The ground-state structure of the 3HIQ monomer was obtained based on the B3LYP functional with TZVP basis set. To evaluate the solvent effect, cyclohexane, compared with the experiment, was selected in the calculations according to the IEF-PCM model. The geometric S_0 for 3HIQ monomer was optimized without constraint of bonds, angles and dihedral angles. Vibrational frequencies were calculated to analyze the optimized structures to confirm that the structures were in the local minima. Vertical excitation energy and the S_1 structure of the 3HIQ monomer was performed based on the ground optimized structure using the TDDFT method IEF-PCM solvation model. The calculated absorption and fluorescence spectra are shown in Fig. 1. It could be clearly seen that the strong absorption peak for the 3HIQ enol form (3HIQ-E) is at 323 nm in cyclohexane, which is in consistent with the experimental value (340 nm) ^[49]. Moreover, the fluorescence spectrum of 3HIQ-E* reveals a normal Stokes shifted emission maximum at 364 nm, which is consistent with the experimental value (370 nm) ^[49]. This further illustrates the rationality of the calculated method we have adopted.

Based on the DFT method and previous work ^[27], we carried out structural optimization with a fixed O–H bond distance ranging from 0.97 Å to 2.77 Å and constructed the ground-state potential energy curve of 3HIQ-E based on the B3LYP functional with TZVP basis set as shown in Fig. 2. All the stationary points along the reaction coordinate were full frequency analyses. We took the energy of the initial configuration as the zero point energy. It should be noted that there exists a high barrier (~37.023 kcal/mol) between 3HIQ-E and the 3HIQ keto form (3HIQ-K), and the O–H bond length of the stationary point of 3HIQ-K is 2.432 Å. The high barrier prevents the hydrogen atom of the 3HIQ-E hydroxy group from overlapping and forming 3HIQ-K. That is to say, the transformation of the 3HIQ-K monomer in the ground state to the 3HIQ-E form is difficult, which further demonstrates that the keto/enol form is difficult to exist during 3HIQ self-association.

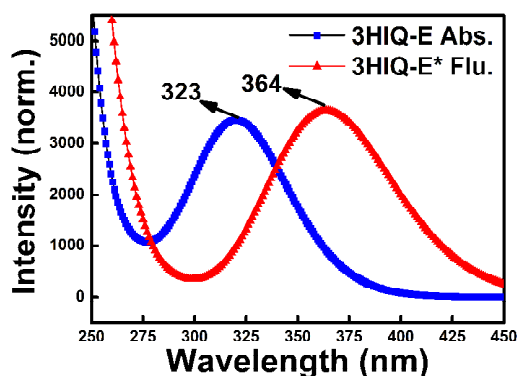


Fig. 1 The calculated absorption and fluorescence spectra of the 3HIQ monomer at the TDDFT/B3LYP/TZVP level.

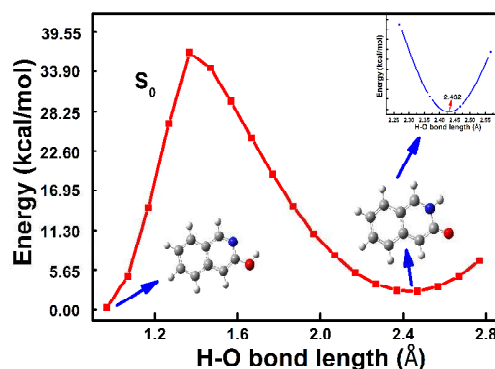


Fig. 2 Potential energy curve for the S_0 state in the 3HIQ-E form along with O–H bond length, and the inset shows the detailed potential energy curve of the 3HIQ-K configuration.

3.2 The 3HIQ dimer

The ground and excited state structures of 3HIQ self-association were obtained using the B3LYP functional and TZVP basis set (described in Fig. 3), with cyclohexane selected in the calculations according to the IEF-PCM solvation model. The local minima only have real frequencies based on vibrational frequency analysis. In order to show our illustration more conveniently, we labeled serial numbers on the atoms connected to the hydrogen bonds. In addition, the primary bond lengths (Å) and angles (°) of 3HIQ self-association in the ground state and first excited state by DFT and TDDFT methods are listed in Table 1. In our calculations, we found three kinds of structures during 3HIQ self-association: the enol/enol form, enol/enol-T (i.e. only one proton transfer form) and keto/keto form. It should be noted that the calculated bond lengths of O_1-H_2 , H_2-N_3 ($H\cdots N$), O_4-H_5 and H_5-N_6 ($H\cdots N$) of enol/enol form are 1.004, 1.746, 1.004 and 1.746 Å, respectively. Upon excitation to the S_1 state, these bond lengths change to 1.004, 1.693, 1.004 and 1.723 Å, respectively. Obviously, the hydrogen bonds ($H_2\cdots N_3$ and $H_5\cdots N_6$) were shortened, which indicates that the intermolecular hydrogen bonds $O_1-H_2\cdots N_3$ and $O_4-H_5\cdots N_6$ are strengthened in the S_1 state.

The first singlet transition ($S_0 \rightarrow S_1$) of the 3HIQ enol/enol corresponds to the orbital transition from the highest occupied molecular orbital (HOMO) to the lowest unoccupied molecular orbital (LUMO). Fig. 4 shows the frontier molecular orbitals for the 3HIQ enol/enol form. It is obvious that the S_1 state is due to a distinct $\pi-\pi^*$ feature. In addition, the electron density of the hydroxyl moiety decreases and the N atom increases after transition from the HOMO to LUMO. That is to say, the S_1 state involves the intermolecular charge transfer and the change of electron density in the hydroxyl moiety can directly influence the intermolecular hydrogen bonding ($O-H\cdots N$). And the increased electron density of nitrogen atoms can enhance the intermolecular hydrogen bonds and promote proton transfer. From the viewpoint of valence bond theory, the interaction between the lone pair of the nitrogen atom and the O–H σ^* orbital is mainly responsible for the proton transfer from the oxygen atom to nitrogen.

Therefore, the excited state proton transfer process may occur due to intermolecular charge transfer.

Table 1 The calculated primary bond lengths (Å) and angles (°) of 3HIQ self-association in the S_0 and S_1 states based on DFT and TDDFT methods, respectively.

Electronic state	3HIQ self-association			
	S_0		S_1	
	enol/enol	keto/keto	enol/enol*	enol/enol-T
O_1-H_2	1.004	1.690	1.004	2.046
H_2-N_3	1.746	1.048	1.693	1.012
O_4-H_5	1.004	1.690	1.004	0.987
H_5-N_6	1.746	1.048	1.723	1.866
$\delta(O_1-H_2-N_3)$	173.2°	179.9°	173.3°	176.3°
$\delta(O_4-H_5-N_6)$	173.2°	179.9°	174.1°	170.6°

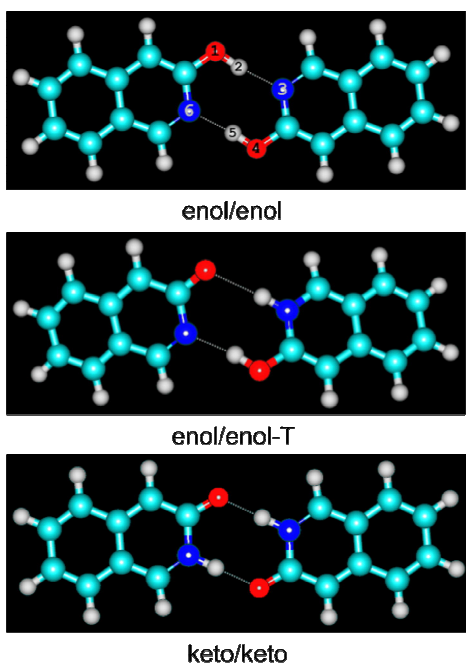


Fig. 3 The optimized structures of the enol/enol form, enol/enol-T form and keto/keto form at the DFT/B3LYP/TZVP calculation level. Red: O; 10 gray: H; blue: N; aqua: C.

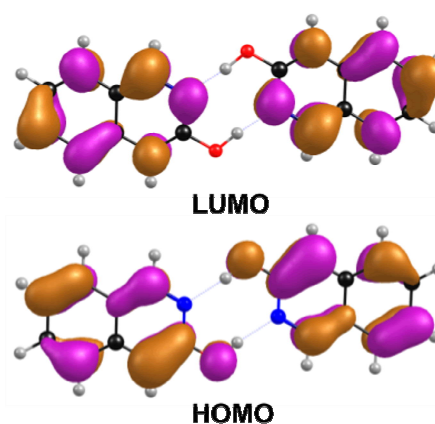


Fig. 4 The calculated frontier molecular orbitals (HOMO and LUMO) of the enol/enol form at the TDDFT/B3LYP/TZVP level.

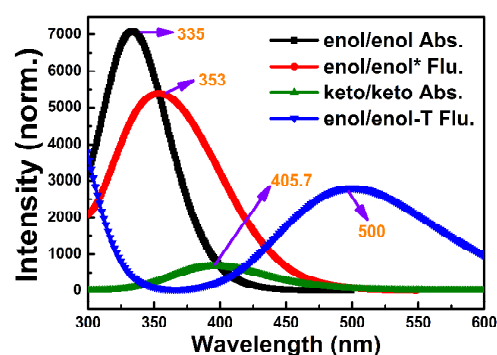


Fig. 5 The calculated absorption and fluorescence spectra of the enol/enol form and enol/enol-T form at the B3LYP/TZVP calculation level.

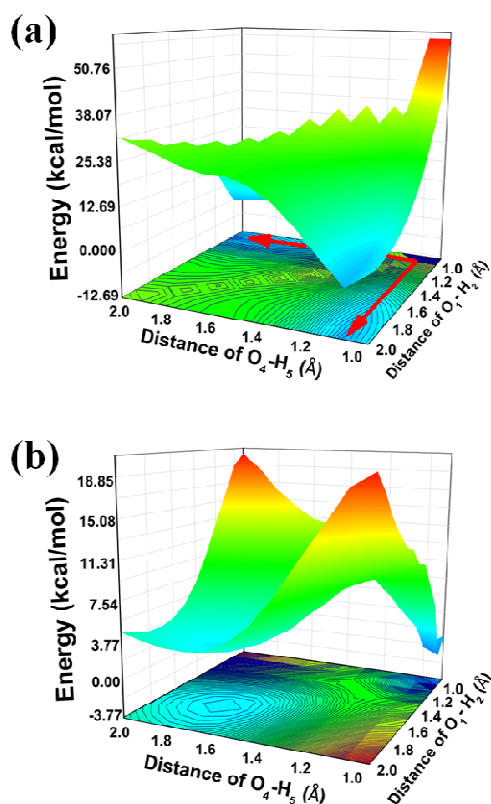


Fig. 6 The constructed PESs on the S_0 and S_1 states as functions of the O_1-H_2 and O_4-H_5 bond lengths both ranging from 0.90 to 2.00 Å among the 3HIQ self-association geometries. (a) S_0 state PES; (b) S_1 state PES. The red arrow indicates the direction of the S_1 state proton transfer process.

Fig. 5 shows the calculated absorption and fluorescence spectra based on the TDDFT/B3LYP/TZVP level. The peak of absorption of the 3HIQ enol/enol was at 335 nm, and the emission peak of the enol/enol form was at 353 nm, both of which agree well with the experimental value^[49]. In addition, the experimental findings also reported another absorption peak at 425 nm, demonstrating that there is another form of 3HIQ self-association existing in the ground state. Because the keto/enol form was difficult to form as described beforehand, we tentatively surmised it was a keto/keto form in the ground state. Further, we calculated the absorption peak of the keto/keto form was at 405.7 nm, which may correspond to the experimental value (425 nm)^[49]. In addition, the emission peak at 490 nm reported experimentally was consistent with the fluorescence peak at 500 nm of the enol/enol-T form (see Fig. 3). Therefore, we speculated that the keto/keto form may derive from the proton transfer of enol/enol-T form. That is to say, dual proton transfer may occur as follows. Upon excitation, the 3HIQ enol/enol transforms to the enol/enol* form, then only one proton of the hydroxyl group in the enol/enol* transfers from the O atom to the N atom forming the enol/enol-T. In turn, through the process of radiative transition, it returns to the ground state and allows the other proton transfer to occur forming the keto/keto structure. So, perhaps it is the only way to form the keto/keto structure in the ground state.

To further reveal more features of the dual proton transfer

process, we optimized all the ground-state and excited-state geometrical structures with fixed O_1-H_2 and O_4-H_5 lengths at the DFT/B3LYP/TZVP level with the IEF-PCM solvation model of cyclohexane under the enlightenment of reference 27. The constructed PESs in the S_0 and S_1 states as functions of the O_1-H_2 and O_4-H_5 lengths (from 0.90 to 2.00 Å) are shown in Fig. 6. Although the TDDFT/B3LYP method can not be expected to be sufficiently accurate to yield the correct ordering of the closely spaced excited state, previous calculations have indicated that the method may be reliable to provide qualitative energetic pathways for the intermolecular proton transfer process^[63-65]. The minimum energies of both the S_0 and S_1 states PESs were selected as the zero point energy. The S_0 state PES is symmetrical as shown in Fig. 6(b), which shows two minimum points: one is the initial 3HIQ enol/enol structure, and the other is the 3HIQ keto/keto form with a coordinate of (1.70 Å, 1.70 Å). In the S_1 state, it should be noted that the PES is also symmetrical (see Fig. 6(a)). Along with the increment of O_1-H_2 and O_4-H_5 bond lengths, it can be seen that the proton transfer process is not synergetic. That is to say, only one proton can transfer from the O atom to N atom forming the enol/enol-T form (primary bond lengths and angles are listed in Table 1). Then, through the process of radiative transition, it returns to the ground state. In turn, the other proton began to transfer through a barrierless process to form the keto/keto structure or the enol/enol structure. In addition, we calculated the potential barrier between the enol/enol form and keto/keto form, which is about 8.98 kcal/mol. In other words, to form the keto/keto structure, it has to undergo a relatively lower barrier of 8.98 kcal/mol from the enol/enol form. It suggests that the keto/keto structure exists in the ground state. Moreover, the 18.965 kcal/mol bond energy of the dihydrogen bonds in the keto/keto form has also been calculated, which is difficult to break and form the keto monomer. Hence, the enol/keto form of 3HIQ self-association reported by Wei *et al.* should be an inaccurate expectation^[49]. So the point that the 425 nm peak is actually ascribed as the absorption peak of the keto/keto structure has been further confirmed. We concluded the dual proton transfer process as follows. The 3HIQ enol/enol turned to the enol/enol* form upon excitation, then only one proton of the hydroxyl group in the enol/enol* form transfers from the O atom to the N atom along the hydrogen bond forming the enol/enol-T form. In turn, through the process of radiative transition, it returns to the ground state and allows the other proton transfer to occur forming the keto/keto structure or regressing to the enol/enol structure.

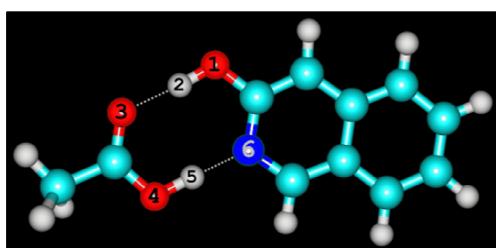
3.3 3HIQ/ACID

The S_0 structures of 3HIQ/ACID were obtained based on the B3LYP functional with TZVP basis set, and subsequent vibrational frequency analysis further confirmed these structures were at the minima (see Fig. 7). To evaluate the solvent effect, ACID was used in the calculations according to the IEF-PCM solvation model. Some of the most important structural parameters have been collected in Table 2. It should be noted that the calculated bond lengths of O_1-H_2 , H_2-O_3 ($H\cdots O$), O_4-H_5 and H_5-N_6 ($H\cdots N$) in the 3HIQ/ACID E-form are 0.992, 1.715, 1.022 and 1.674 Å, respectively. Upon excitation to the S_1 state, these bond lengths are 1.018, 1.575, 1.049 and 1.565, respectively.

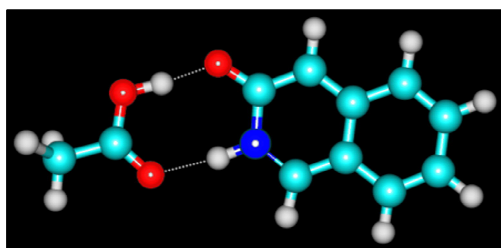
Obviously, the hydrogen bonds ($H_2\cdots O_3$ and $H_5\cdots N_6$) were shortened, while the bond lengths of O_1-H_2 and O_4-H_5 were elongated. These indicate that the intermolecular hydrogen bonds $O_1-H_2\cdots O_3$ and $O_4-H_5\cdots N_6$ are strengthened in the 3HIQ/ACID S_1 E^* -form. The phenomenon of hydrogen bond strengthening can be also explained by monitoring the spectral shifts of some characteristic vibrational modes involved in the formations of hydrogen bonds. Vibrational frequency analysis demonstrated that the formation of the intermolecular hydrogen bonds $O_1-H_2\cdots O_3$ and $O_4-H_5\cdots N_6$ induced a large red-shift of the O_1-H_2 and O_4-H_5 stretching frequency (see Fig. 8). In detail, the stretching frequency of O_1-H_2 was 3261 cm^{-1} in the S_0 state, which was red-shifted to 2809 cm^{-1} in the S_1 state. Moreover, the O_4-H_5 stretching frequency was 2702 cm^{-1} in the S_0 state, whereas in the S_1 state it is 2261 cm^{-1} with a bathochromic shift of 441 cm^{-1} . It is well known that the formation of hydrogen bonds can change the stretching frequencies of both the proton-donating and proton-accepting groups. Further, the stretching vibrational mode is shifted towards a lower frequency and increases its intensity [66,67].

Table 2 The calculated primary bond lengths (\AA) and angles ($^\circ$) of 3HIQ/ACID in the ground state and first excited state by DFT and TDDFT methods, respectively.

Electronic state	3HIQ/ACID			
	S_0	S_1	S_1	S_1
Form	E	K	E^*	K^*
O_1-H_2	0.992	1.555	1.018	1.644
H_2-O_3	1.715	1.024	1.575	1.001
O_4-H_5	1.022	1.801	1.049	1.801
H_5-N_6	1.674	1.033	1.565	1.028
$\delta(O_1-H_2-O_3)$	174.1°	173.9°	175.3°	174.3°
$\delta(O_4-H_5-N_6)$	176.8°	172.6°	178.7°	172.0°



Enol



Keto

Fig. 7 Views of the optimized S_0 structures for 3HIQ/ACID (enol) and 3HIQ/ACID (keto) at the B3LYP/TZVP calculation level. Red: O; gray: H; blue: N; aqua: C.

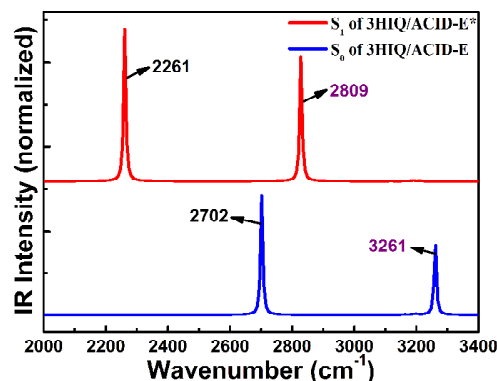


Fig. 8 The calculated IR spectra of hydrogen-bonded 3HIQ/ACID in the spectral region for O-H stretching bands in the S_0 and S_1 states. The purple numbers represent the O_1-H_2 stretching band, and the black numbers represent the O_4-H_5 stretching band.

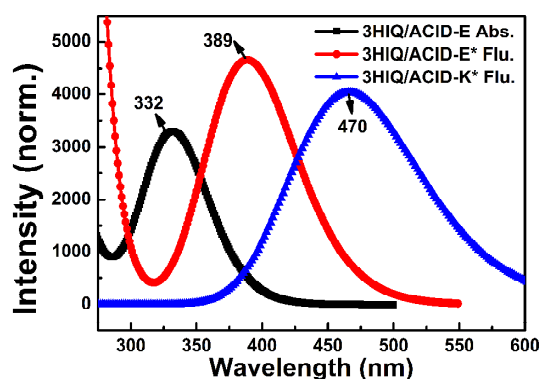


Fig. 9 The calculated absorption and fluorescence spectra of 3HIQ/ACID (enol) and 3HIQ/ACID (keto) at the B3LYP/TZVP calculation level.

The excitation energies and oscillator strengths of the first singlet electronic transitions were calculated based on the TDDFT/B3LYP/TZVP method with IEF-PCM solvation model, and fluorescence spectra were obtained from the optimized S_1 state structures. As shown in Fig. 9, in order to see the shape of the spectra clearly, we depicted the calculated absorption and fluorescence spectra from 275 to 600 nm. It should be clearly found that the absorption peak for 3HIQ/ACID-E was at 332 nm, which is consistent with the experimental value (350 nm) [49]. Upon excitation, there are two fates for the excited state. One is 3HIQ/ACID- E^* , and the other is 3HIQ/ACID- K^* . Through theoretical calculations, the result of 3HIQ/ACID- E^* reveals a normal Stokes shifted emission maximum at 389 nm. In the case of the geometry-relaxed keto form 3HIQ/ACID- K^* , a large Stokes shift upon emissive relaxation was calculated at 470 nm, which is consistent with the experimental fluorescence spectra (490 nm). It further confirmed that 3HIQ/ACID- K^* was the end product in the S_1 state through the PT reaction. Fig. 10 shows the frontier molecular orbitals for 3HIQ/ACID. The first singlet transition ($S_0 \rightarrow S_1$) of 3HIQ/ACID-E corresponds to the orbital

transition from the HOMO to LUMO. Therefore, we only showed the HOMO and LUMO orbitals. The π character for the HOMO as well as the π^* character of the LUMO can be seen clearly. So it was determined that the S_1 state is due to a distinct $\pi-\pi^*$ feature. It is interesting that the σ character of the $N\cdots H$ bond involved in the LUMO of the 3HIQ/ACID- E^* complex suggests a strong electron pair donation ability of the $-N-$ group to form a covalent bond with the H atom of the adjacent AcOH after photoexcitation to the S_1 state. In addition, there is a greater electronic density distribution located around the phenolic oxygen atom of 3HIQ/ACID- E , and less located around nitrogen in the HOMO than that in the LUMO. Therefore, the excited-state 3HIQ/ACID- E^* should favor the keto tautomer by protonation of the $-N-$ group and deprotonation of the phenolic group. Thus, it can be concluded that upon the $S_0 \rightarrow S_1$ (HOMO \rightarrow LUMO) transition, which is quite intense, the enol form (E^*) formed undergoes rapid excited state intermolecular proton transfer with the formation of the excited state keto form (K^*). In many cases the K^* decays to the ground state K through a radiative process following a reverse proton transfer in the ground state. In addition, it should be noted that the electron densities of all the MOs are strictly localized on the 3HIQ moiety. Therefore, it has been confirmed that the ACID stays in its electronic ground state in the whole excited-state proton-transfer process.

In order to reveal more features of the intermolecular proton transfer process in the 3HIQ/ACID mechanism, we optimized all the S_0 state and S_1 state geometrical structures with fixed O_1-H_2 and O_4-H_5 bond lengths at the DFT/B3LYP/TZVP level with the IEF-PCM solvation model of ACID. The constructed PESs in the S_0 and S_1 states as functions of the O_1-H_2 and O_4-H_5 bond lengths ranging from 0.89 to 1.99 Å as well as from 0.92 to 2.02 Å among the 3HIQ/ACID- E and 3HIQ/ACID- K geometries are shown in Fig. 11, respectively. Fig. 11(a) shows that the energy of the S_1 state decreases when lengthening both the O_1-H_2 and O_4-H_5 bond lengths simultaneously, and increases through a stable point at a coordinate of (1.644 Å, 1.801 Å), which is the global minimum in the S_1 PES. In addition, we chose the energy of the stable point as the relative coordinates zero point, which is also just the stable optimized geometry of 3HIQ/ACID- K^* (some of the most important structural parameters are shown in Table 1). Obviously, it is a barrierless PES in the S_1 state and shows the transfer process is synergetic. In addition, it provides a possible explanation for the fluorescence quenching (emission peaks from 389 nm to 470 nm). The energy of 3HIQ/ACID- K^* is about 29.9 kcal/mol lower than 3HIQ/ACID- E^* indicating the dual proton transfer process is exothermic. The S_0 state PES is shown in Fig. 11(b), it can be noted that there is a moderate barrier (~ 9.7 kcal/mol) between 3HIQ/ACID- E and 3HIQ/ACID- K , which means that the proton transfer process in the ground state is not as easy as that in the excited state. Considering these two equilibria in the S_0 state and the PESs mentioned above, we can delineate the mechanism of dual protons transfer as follows: first, the 3HIQ chemosensor formed dual hydrogen bonds with ACID in the ground state. After excitation, the intermolecular hydrogen bonds $O_1-H_2\cdots O_3$ and $O_4-H_5\cdots N_6$ are strengthened in the 3HIQ/ACID- E^* form. Then, strengthened dual hydrogen bonds facilitate the simultaneous dual proton transfer process to form the 3HIQ/ACID- K^* structure. Consequently, the 3HIQ/ACID- K^*

decays to the ground state 3HIQ/ACID- K form through radiating fluorescence, which is quenched due to the dual proton transfer process.

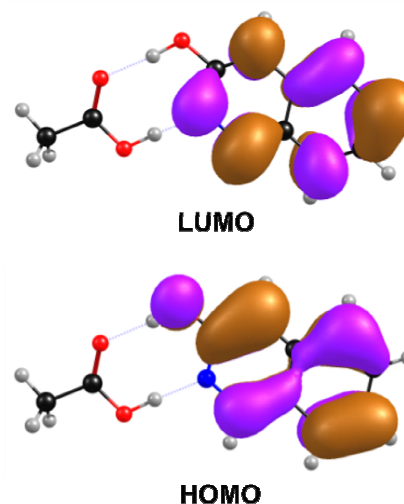


Fig. 10 The calculated frontier molecular orbitals (HOMO and LUMO) of 3HIQ/ACID at the TDDFT/B3LYP/TZVP level.

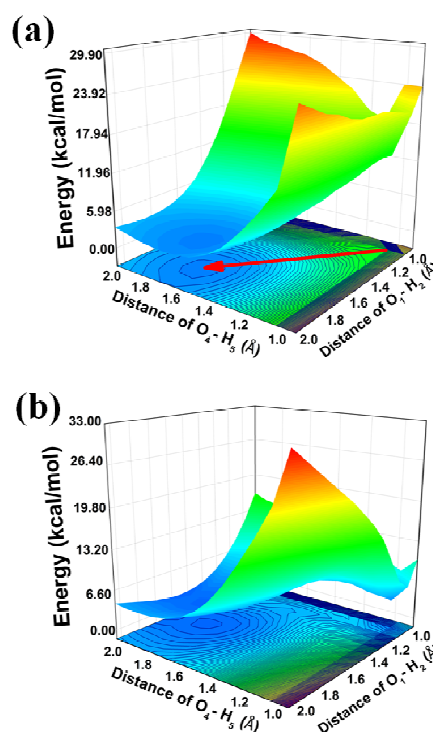


Fig. 11 The constructed PESs on the S_0 and S_1 states as functions of the O_1-H_2 and O_4-H_5 bond lengths ranging from 0.89 to 1.99 Å as well as from 0.92 to 2.02 Å among the 3HIQ/ACID- E and 3HIQ/ACID- K geometries, respectively. (a) S_0 state PES; (b) S_1 state PES. The red arrow indicates the direction of the S_1 state proton transfer.

4. Conclusion

In summary, we have carried out a detailed excited-state dynamic investigation on the 3HIQ monomer, 3HIQ self-association and 3HIQ/ACID based on the DFT/B3LYP/TZVP

calculation level. Firstly, through investigating the 3HIQ monomer in cyclohexane, we found that the 3HIQ-keto form is difficult to form in the ground state due to the high barrier (37.023 kcal/mol) between the 3HIQ enol form and 3HIQ keto form. Then, we calculated the electronic spectra of 3HIQ self-association in cyclohexane, which agree well with the experimental results. In addition, the 18.965 kcal/mol bond energy of the dual hydrogen bonds of the keto/keto form was calculated, demonstrating that it is difficult to break the dual hydrogen bonds to form the keto monomer. Hence, the enol/keto form of 3HIQ self-association reported by Wei *et al.* should be an inaccurate expectation^[49]. The constructed PESs of the S_0 and S_1 states demonstrate the proton transfer mechanism for 3HIQ self-association. In detail, the 3HIQ enol/enol form is excited to the first excited state, then transfers one proton to form the 3HIQ enol/enol-T form. In turn, it radiates transition to the ground state to transfer another proton. Two stable structures of 3HIQ self-association (3HIQ enol/enol form and 3HIQ keto/keto form) can both exist in the ground state because of the relatively low barrier (8.98 kcal/mol). In addition, we selected the ACID solvent to further study the process of proton transfer of 3HIQ/ACID. The present TDDFT calculations reproduced the experimental absorption and fluorescence spectra well. In the same constructed PES method, we found the dual proton transfer in the first excited state synergistically, differ from 3HIQ self-association. In addition, both two proton transfer mechanisms can provide a reasonable explanation for the fluorescence quenching phenomenon observed experimentally.

Acknowledgements

This work was financially supported by the National Natural Science Foundation of China (Grant No. 11304135, 11374353 and 21271095), the Doctor Subject Foundation of the Ministry of Education of China (20132101110001), the Liaoning Natural Science Foundation of China (2013020100 and 2013004003). F.C. Ma is indebted to the support from the Program of Liaoning Key Laboratory of Semiconductor Light Emitting and Photocatalytic Materials.

References

- 1 W. M. Kwok, C. Ma and D. L. Phillips, *J. Am. Chem. Soc.*, 2008, 130, 5131
- 2 G. J. Zhao, K. L. Han and P. J. Stang, *J. Chem. Theory Comput.*, 2009, 5, 1955.
- 3 S. B. Suh, J. C. Kim, Y. C. Choi, G. Yun and K. S. Kim, *J. Am. Chem. Soc.*, 2004, 126, 2186.
- 4 K. L. Han, G. Z. He and N. Q. Lou, *J. Chem. Phys.*, 1996, 105, 8699.
- 5 D. M. Li, X. Q. Huang, K. L. Han and C. G. Zhan, *J. Am. Chem. Soc.*, 2011, 133, 7416.
- 6 G. J. Zhao, J. Y. Liu, L. C. Zhou and K. L. Han, *J. Phys. Chem. B*, 2007, 111, 8940.
- 7 G. J. Zhao and K. L. Han, *J. Phys. Chem. A*, 2009, 113, 14329.
- 8 D. Sicinska, D. G. Truhlar and P. Paneth, *J. Am. Chem. Soc.*, 2001, 123, 7683.
- 9 G. J. Zhao and K. L. Han, *J. Comput. Chem.*, 2008, 29, 2010.
- 10 G. J. Zhao and K. L. Han, *Biophys. J.*, 2008, 94, 38.

- 11 G. J. Zhao and K. L. Han, *Phys. Chem. Chem. Phys.*, 2010, 12, 8914.
- 12 M. T. Sun, *J. Chem. Phys.* 2006, 124, 054903.
- 13 J. F. Zhao, P. Song, Y. L. Cui, X. M. Liu, S. W. Sun, S. Y. Hou and F. C. Ma, *Spectrochim. Acta Part A*, 2014, 131, 282.
- 14 M. T. Sun, Z. L. Zhang, H. R. Zheng and H. X. Xu, *Science Reports.*, 2012, 2, 1.
- 15 N. Kumari, S. Jha and S. Bhattacharya, *J. Org. Chem.*, 2011, 76, 8215.
- 16 Z. C. Wen and Y. B. Jiang, *Tetrahedron.*, 2004, 60, 11109.
- 17 X. J. Peng, Y. K. Wu, J. L. Fan, M. Z. Tian and K. L. Han, *J. Org. Chem.*, 2005, 70, 10524.
- 18 G. Y. Li, G. J. Zhao, Y. H. Liu, K. L. Han and G. Z. He, *J. Comput. Chem.*, 2010, 31, 1759.
- 19 G. Y. Li and T. S. Chu, *Phys. Chem. Chem. Phys.*, 2011, 13, 20766.
- 20 W. J. Xu, S. J. Liu, H. B. Sun, X. Y. Zhao, Q. Zhao, S. Sun, S. Cheng, T. C. Ma, L. X. Zhou and W. Huang, *J. Mater. Chem.*, 2011, 21, 7572.
- 21 P. Jaramillo, K. Coutinho and S. Canuto, *J. Phys. Chem. A*, 2009, 113, 12485.
- 22 D. A. Dybala, P. Paneth, J. Z. Pu and D. G. Truhlar, *J. Phys. Chem. A*, 2004, 108, 2475.
- 23 M. Pietrzak, M. F. Shibl, M. Broring, O. Kuhn and H. H. Limbach, *J. Am. Chem. Soc.*, 2007, 129, 296.
- 24 K. L. Han and G. Z. He, *J. Photochem. Photobiol. C. Photochem. Rev.*, 2007, 8, 55.
- 25 A. Weller, *Z. Z. Elektrochem.*, 1956, 60, 1144.
- 26 A. Mordzinski, A. Grabowska, W. Kuhnle and A. Krowczynski, *Chem. Phys. Lett.*, 1983, 101, 291.
- 27 S. Chai, G. J. Zhao, P. Song, S. Q. Yang, J. Y. Liu and K. L. Han, *Phys. Chem. Chem. Phys.*, 2009, 11, 4385.
- 28 A. Sytnik and M. Kasha, *Proc. Natl. Acad. Sci. U.S.A.*, 1994, 91, 8627.
- 29 Y. Kubo, S. Maeda, S. Tokita and M. Kubo, *Nature*, 1996, 382, 522.
- 30 F. B. Yu, P. Li, G. J. Zhao, T. S. Chu and K. L. Han, *J. Am. Chem. Soc.*, 2011, 133, 11030.
- 31 F. B. Yu, P. Li, B. S. Wang and K. L. Han, *J. Am. Chem. Soc.*, 2013, 20, 7674.
- 32 J. S. Chen, P. W. Zhou, S. Q. Yang, A. P. Fu and T. S. Chu, *Phys. Chem. Chem. Phys.*, 2013, 10, 1039.
- 33 P. T. Chou, M. L. Martinez, W. C. Cooper and C. P. Chang, *Appl. Spectrosc.*, 1994, 48, 604.
- 34 D. G. Ma, F. S. Liang, L. X. Wang, S. T. Lee and L. S. Hung, *Chem. Phys. Lett.*, 2002, 358, 24.
- 35 P. T. Chou, S. L. Studer and M. L. Martinez, *Appl. Spectrosc.*, 1991, 45, 513.
- 36 J. Catalan, J. C. Delvalle, F. Fabero and N. A. Garcia, *Photochem. Photobiol.*, 1995, 61, 118.

- 37 P. T. Chou, M. L. Martinez and S. L. Studer, *Appl. Spectrosc.*, 1991, 45, 918.
- 38 J. Keck, H. E. A. Kramer, H. Port, T. Hirsch, P. Fischer and G. Rytz, *J. Phys. Chem.*, 1996, 100, 144468.
- 5 39 B. Feringa, *Ed. Wiley-VCH: Weinheim, Germany*, 2001.
- 40 Memories and Switches, *Special issue of Chem. Rev.* 2000, 100.
- 41 M. S. Mehata, *J. Phys. Chem. B.*, 2008, 112, 8383.
- 42 P. T. Chou, C. Y. Wei and F. T. Hung, *J. Phys. Chem. A.*, 1999, 103, 1939.
- 10 43 Y. H. Liu and S. C. Lan, *Commun. Comput. Chem.*, 2013, 1, 1.
- 44 H. L. Ammon and G. L. Wheeler, *Acta Crystallogr.*, 1974, B30, 1146.
- 45 D. A. Evans, G. F. Smith and M. A. Wahid, *J. Chem. Soc. B.*, 1967, 590.
- 15 46 R. T. Hendricks, *Bioorg. Med. Chem. Letter.*, 2009, 19, 410.
- 47 K. M. Allan, B. D. Hong and B. M. Stoltz, *Org. Biomol. Chem.*, 2009, 7, 4960.
- 48 N. R. Nimlos, D. F. Kelley and E. R. Bernstein, *J. Phys. Chem.*, 1989, 93, 643.
- 20 49 C. Y. Wei, W. S. Yu and P. T. Chou, *J. Phys. Chem. B.*, 1998, 102, 1053.
- 50 A. D. Becke, *J. Chem. Phys.*, 1993, 98, 5648.
- 51 C. T. Lee, W. T. Yang and R. G. Parr, *Phys. Rev. B: Condens. Matter Mater. Phys.*, 1988, 37, 785.
- 25 52 B. Miehlich, A. Savin, H. Stoll and H. Preuss, *Chem. Phys. Lett.*, 1989, 157, 200.
- 53 A. Schafer, H. Horn and R. Ahlrichs, *J. Chem. Phys.*, 1992, 97, 2571.
- 54 A. Schafer, C. Huber and R. Ahlrichs, *J. Chem. Phys.*, 1994, 100, 5829.
- 30 55 M. J. Frisch, G. W. Trucks, H. B. Schlegel, G. E. Scuseria, M. A. Robb, J. R. Cheeseman, G. Scalmani, V. Barone, B. Mennucci, G. A. Petersson, H. Nakatsuji, M. Caricato, X. Li, H. P. Hratchian, A. F. Izmaylov, J. Bloino, G. Zheng, J. L. Sonnenberg, M. Hada, M. Ehara, K. Toyota, R. Fukuda, J. Hasegawa, M. Ishida, T. Nakajima, Y. Honda, O. Kitao, H. Nakai, T. Vreven, J. A. Montgomery Jr, J. E. Peralta, F. Ogliaro, M. Bearpark, J. J. Heyd, E. Brothers, K. N. Kudin, V. N. Staroverov, T. Keith, R. Kobayashi, J. Normand, K. Raghavachari, A. Rendell, J. C. Burant, S. S. Iyengar, J. Tomasi, M. Cossi, N. Rega, J. M. Millam, M. Klene, J. E. Knox, J. B. Cross, V. Bakken, C. Adamo, J. Jaramillo, R. Gomperts, R. E. Stratmann, O. Yazyev, A. J. Austin, R. Cammi, C. Pomelli, J. W. Ochterski, R. L. Martin, K. Morokuma, V. G. Zakrzewski, G. A. Voth, P. Salvador, J. J. Dannenberg, S. Dapprich, A. D. Daniels, O. Farkas, J. B. Foresman, J. V. Ortiz, J. Cioslowski and D. J. Fox, Gaussian, Inc., Wallingford, CT, 2010.
- 45 56 B. Mennucci, E. Cancès and J. Tomasi, *J. Phys. Chem. B.*, 1997, 101, 10506.
- 57 E. Cancès, B. Mennucci and J. Tomasi, *J. Chem. Phys.*, 1997, 107, 3032.
- 50 58 R. Cammi and J. Tomasi, *J. Comput. Chem.*, 1995, 16, 1449.
- 59 S. Miertus, E. Scrocco and J. Tomasi, *J. Chem. Phys.*, 1981, 55, 117.
- 60 G. J. Zhao and K. L. Han, *ChemPhysChem.*, 2008, 9, 1842.
- 61 G. J. Zhao and K. L. Han, *J. Phys. Chem. A.*, 2007, 111, 9218.
- 62 F. Furche and R. Ahlrichs, *J. Chem. Phys.*, 2002, 117, 7433.
- 55 63 A. L. Sobolewski and W. Domcke, *Phys. Chem. Chem. Phys.*, 1999, 1, 3065.
- 64 A. L. Serrano and M. Merchán, *J. Photochem. Photobio. C Photochem. Rev.*, 2009, 10, 21.
- 65 Y. Sags, Y. Shibata and H. Tamiaki, *J. Photochem. Photobio. C Photochem. Rev.*, 2010, 11, 15.
- 60 66 G. J. Zhao and K. L. Han, *Acc. Chem. Res.*, 2012, 45, 404.
- 67 P. Song and F. C. Ma, *International Reviews in Physical Chemistry.*, 2013, 32, 589.